Biochemical Pharmacology 79 (2010) 1506–1515

Contents lists available at ScienceDirect

Biochemical Pharmacology

journal homepage: www.elsevier.com/locate/biochempharm

Blockade of LTB_4-induced chemotaxis by bioactive molecules interfering with the BLT2-$G\alpha_i$ interaction

Joo-Young Kim [a,1], Won-Kyu Lee [b,1], Yeon Gyu Yu [b,**], Jae-Hong Kim [a,*]

[a] School of Life Sciences and Biotechnology, Korea University, Seoul 136-701, Republic of Korea
[b] Department of Chemistry, Kookmin University, Seoul 136-702, Republic of Korea

ARTICLE INFO

Article history:
Received 13 November 2009
Accepted 13 January 2010

Keywords:
Chemotaxis
LTB_4
BLT2
Purpurin
Chloranil

ABSTRACT

BLT2, a low-affinity leukotriene B_4 (LTB_4) receptor, is a member of the G-protein coupled receptor (GPCR) family and is involved in the pathogenesis of inflammatory diseases such as asthma. Despite its clinical implications, however, no pharmacological inhibitors are available. In the present study, we screened for small molecules that interfere with the interaction between the third intracellular loop region of BLT2 ($BLT2_{iL3}$) and the $G\alpha_{i3}$ protein subunit ($G\alpha_{i3}$), using a high-throughput screening (HTS) assay with a library of 1040 FDA-approved drugs and bioactive compounds. We identified two small molecules—purpurin [1,2,4-trihydroxy-9,10-anthraquinone; IC_{50} = 1.6 μM for BLT2] and chloranil [tetrachloro-1,4-benzoquinone; IC_{50} = 0.42 μM for BLT2]—as specific BLT2-blocking agents. We found that blockade of the $BLT2_{iL3}$-$G\alpha_{i3}$ interaction by these small molecules inhibited the BLT2-downstream signaling cascade. For example, BLT2-signaling to phosphoinositide-3 kinase (PI3K)/Akt phosphorylation was completely abolished by these molecules. Furthermore, we observed that these small molecules blocked LTB_4-induced chemotaxis by inhibiting the BLT2-PI3K/Akt-downstream, Rac1-reactive oxygen species-dependent pathway. Taken together, our results show that purpurin and chloranil interfere with the interaction between $BLT2_{iL3}$ and $G\alpha_{i3}$ and thus block the biological functions of BLT2 (e.g., chemotaxis). The present findings suggest a potential application of purpurin and chloranil as pharmacological therapeutic agents against BLT2-associated inflammatory human diseases.

1. Introduction

Leukotriene B_4 (LTB_4), a lipid metabolite of arachidonic acid (AA), is one of the most potent chemotactic mediators for the recruitment of leukocytes [1,2]. Although LTB_4-mediated leukocyte recruitment has a protective role against various pathogens [3], it is also involved in the pathogenesis of such inflammatory diseases as bronchial asthma [4], rheumatoid arthritis [5], atherosclerosis [6], and inflammatory bowel disease [7]. Therefore, antagonists for LTB_4 receptors have recently been under development as potent anti-inflammatory drugs. LTB_4 exerts its biological effects via two G-protein coupled receptors (GPCRs), BLT1 and BLT2 [1,8]. Most studies of LTB_4 receptors have focused on the high-affinity receptor BLT1, which is expressed exclusively in inflammatory cells such as leukocytes and plays a role in inflammatory processes [1,9].

In contrast, BLT2, a low-affinity receptor for LTB_4, is expressed in a wide variety of tissues [8,10]. Although no clear physiological function has yet been identified for BLT2, recent studies have demonstrated that it is involved in various inflammatory disorders such as asthma [11], atherosclerosis [6], and cancer progression [12,13]. It is well known that BLT2 is involved in calcium mobilization and chemotactic migration in cells under LTB_4 stimulus. Furthermore, LTB_4 and Compound A [4′-pentanoyl (phenyl) amino methyl-1,1′-biphenyl-2-carboxylic acid], a specific agonist of BLT2, induce chemotactic migration in primary mouse keratinocytes [14]. In addition, Shin et al. recently reported that LTB_4-induced dendritic cell (DC) chemotaxis was mediated in a BLT2-dependent manner via phosphoinositide-3 kinase (PI3K)/Akt pathway and was completely inhibited by pretreatment with pertussis toxin (PTX) [15], suggesting that the $G\alpha_i$ or $G\alpha_o$ protein subunit may be involved in the BLT2-mediated chemotactic response. Previously, we have dissected the interaction between BLT2 and various types of Gα subunits of the G_i family, using different intracellular domains of BLT2, and revealed that the third intracellular loop region ($BLT2_{iL3}$) of BLT2 makes a specific interaction with $G\alpha_{i3}$ [16]. Therefore, specific inhibitors that block the interaction between BLT2 and $G\alpha_{i3}$ may inhibit LTB_4-BLT2-mediated signaling (e.g., chemotaxis) and ameliorate BLT2-associated inflammatory diseases.

* Corresponding author. Tel.: +82 2 3290 3452; fax: +82 2 927 9028.
** Corresponding author. Tel.: +82 2 910 4619; fax: +82 2 910 4415.
E-mail addresses: ygyu@kookmin.ac.kr (Y.G. Yu), jhongkim@korea.ac.kr (J.-H. Kim).
[1] Both authors contributed equally (co-first authors).

0006-2952/$ – see front matter © 2010 Elsevier Inc. All rights reserved.
doi:10.1016/j.bcp.2010.01.018

With this in mind, we performed high-throughput screening (HTS) using a library (NINDS collection of 1040 compounds) composed of FDA-approved drugs and bioactive compounds in order to identify specific molecules that could interfere with the binding of BLT2 and $G\alpha_{i3}$ proteins. This library has been used to screen therapeutic agents against neurological disorders including Huntington disease [17] and amyotrophic lateral sclerosis [18], and recently its application has been extended to screening therapeutic agents against prostate cancer progression and metastasis [19] and against hair cell loss [20]. In the present study, we identified two small molecules specifically interfering with the interaction between BLT2 [via the third intracellular loop region of BLT2 ($BLT2_{iL3}$)] and the $G\alpha_i$ protein subunit [$G\alpha_{i3}$ subunit ($G\alpha_{i3}$)]. Additionally, we demonstrated that LTB_4-BLT2-downstream signaling components (e.g., PI3K/Akt, Rac1, and ROS) are also specifically inhibited by purpurin and chloranil, thus attenuating LTB_4-BLT2-mediated signaling to chemotaxis.

2. Materials and methods

2.1. Chemicals, reagents and plasmids

Triton X-100, lauryldimethylamine N-oxide (LDAO), and *n*-Octyl-β-D-glucopyranoside (OG) were obtained from Sigma–Aldrich (St. Louis, MO). The NINDS Custom Collection II (Micro-Source Discovery System, CT) of 1040 biologically active compounds was used in the screening process. The human cDNA library was purchased from Novagen (Madison, WI). 2′,7′-dichlorodihydrofluorescein diacetate (H_2DCFDA) was purchased from Molecular Probes (Eugene, OR). LTB_4 was purchased from Cayman (Ann Arbor, MI). LY294002 and NAC were purchased from Sigma–Aldrich. PTX, PD98059, and Geneticin (G418) were purchased from Calbiochem (San Diego, CA). Fetal bovine serum (FBS), RPMI 1640, and phenol red-free RPMI 1640 were purchased from Invitrogen (Carlsbad, CA). All other chemicals were acquired from standard sources and were of molecular biology grade or higher. The hBLT1 plasmid was obtained from Dr. Shimizu (University of Tokyo, Tokyo, Japan), and the hBLT2 (GenBank accession no. NM019839) plasmid was cloned by PCR using a human genomic bacterial artificial chromosome (BAC) library, as previously described for other chemoattractant receptors, with minor modifications in PCR conditions [21]. The BAC library was a kind gift from Dr. Young-Chul Choi (Kyung Hee University, Korea). The pcDNA3.1 and pET22b vectors were purchased from Invitrogen and Novagen, respectively.

2.2. Cell culture

CHO cells were obtained from the Korean Cell Line Bank (KCLB, 10061), and the cells were grown in RPMI 1640 supplemented with 10% FBS, penicillin (50 units/mL), and streptomycin (50 μg/mL) at 37 °C under a humidified 95%, 5% (v/v) mixture of air and CO_2. Stable cells (CHO-vector, CHO-BLT1, and CHO-BLT2) were prepared and maintained in the media with 0.5 mg/mL G418.

2.3. Preparation of GST-$BLT2_{iL3}$ and His-$G\alpha_{i3}$

The expression vectors for the third intracellular loop region of BLT2 ($BLT2_{iL3}$) and $G\alpha_{i3}$ have been described previously [16]. The pGST-$BLT2_{iL3}$ plasmid contains $BLT2_{iL3}$ (amino acids 237–256 of BLT2) at the C-terminus of GST in pET22b, and pHis-$G\alpha_{i3}$ was used for the expression of $G\alpha_{i3}$ containing a 6×-His tag at its N-terminus (Fig. 1B and C).

GST-$BLT2_{iL3}$ and His-$G\alpha_{i3}$ were prepared as previously described [16]. Briefly, *Escherichia coli* Rosetta 2 (DE3) cells harboring the GST-$BLT2_{iL3}$ or His-$G\alpha_{i3}$ expression plasmid were grown in LB medium to an optical density (O.D.) of 0.7 at 600 nm. The expression of GST-$BLT2_{iL3}$ or His-$G\alpha_{i3}$ was induced by adding 1 mM isopropyl-β-D-thiogalactopyranoside (IPTG) for 4 h or 16 h, respectively, at 37 °C in LB medium containing 50 μg/mL

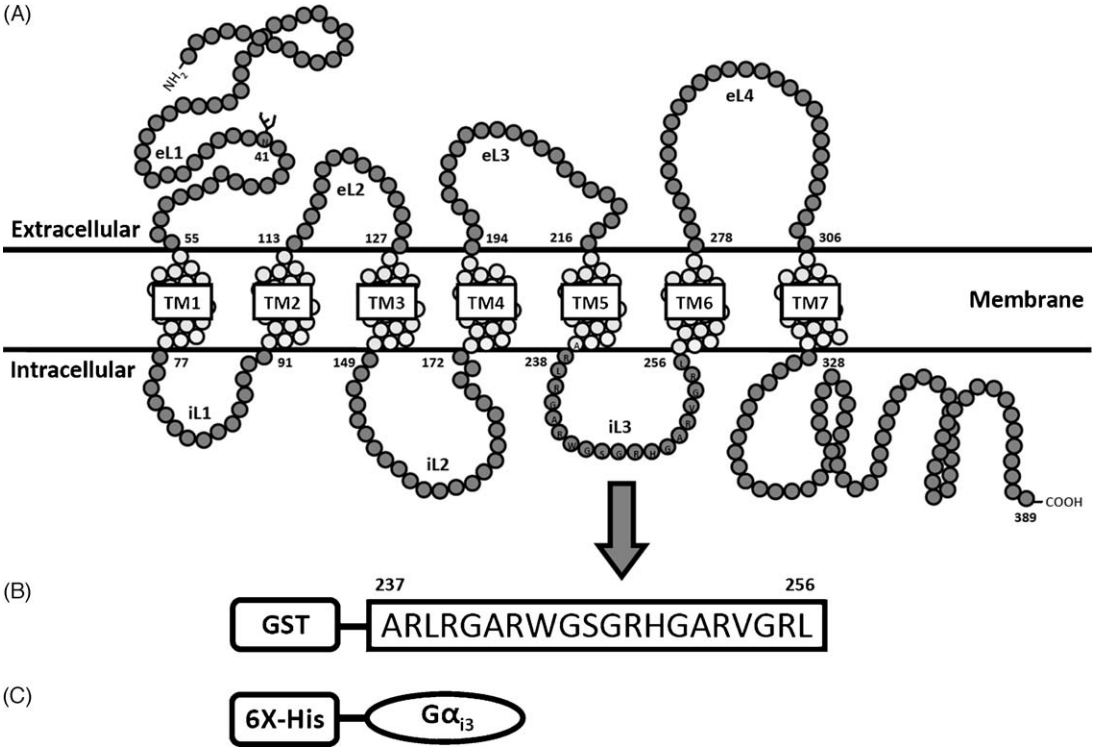

Fig. 1. Schematic representation of human BLT2, GST-$BLT2_{iL3}$, and His-$G\alpha_{i3}$. (A) Human BLT2 diagram showing a schematic topology (GenBank accession no. NM019839; UniProtKB/Swiss-Prot accession no. Q9NPC1). (B) GST-$BLT2_{iL3}$ describes the iL3 region of BLT2 containing the GST tag at the N-terminus. The third intracellular loop (iL3) region represents amino acids 237–256 of BLT2 and is indicated by a box. (C) His-$G\alpha_{i3}$ represents $G\alpha_{i3}$ proteins containing the 6×-His tag at the N-terminus.

ampicillin. GST-BLT2$_{iL3}$ and His-Gα_{i3} were purified from the subsequent cell lysate by affinity purification using a glutathione affinity resin column (Peptron Inc, Korea) or by immobilized metal chelating chromatography (IMAC) using Ni-NTA (Qiagen, Germany), respectively. The glutathione and imidazole in the purified protein samples were removed with desalting columns (GE Healthcare, WI), and the proteins were stored at −80 °C until further analysis.

2.4. Measurement of the interaction between GST-BLT2$_{iL3}$ and FITC-His-Gα_{i3}

His-Gα_{i3} was covalently labeled with flourescein isothiocyanate (FITC) according to the manufacturer's manual (Sigma–Aldrich). The interaction between GST-BLT2$_{iL3}$ and FITC-His-Gα_{i3} was analyzed by measuring the amount of FITC-His-Gα_{i3} bound to GST-BLT2$_{iL3}$ immobilized on a glutathione plate (Pierce), as previously described [16]. Briefly, 1 μM of GST-BLT2$_{iL3}$ protein in PBS (50 mM sodium phosphate, pH 7.4, and 200 mM NaCl) was immobilized on the glutathione plate, and the plate was incubated with FITC-labeled His-Gα_{i3} (100 μL per well). The specifically bound FITC-labeled His-Gα_{i3} proteins were eluted with 8 M urea, and the intensity of fluorescence from the eluted FITC-His-Gα_{i3} was measured at excitation and emission wavelengths of 495 and 525 nm, respectively, using a TRIAD microplate reader (Dynex Technologies, VA). The percentage of inhibition was calculated using the equation $(A_o - A)/A_o \times 100$ (%), where A and A_o were the absorbance values at 495 nm of the reaction mixtures with or without chemical compounds, respectively. For the screening of compounds (from the NINDS chemical library) that could interfere with the interaction between GST-BLT2$_{iL3}$ and His-Gα_{i3}, 50 μM of each compound was incubated along with FITC-labeled His-Gα_{i3} during the measurement.

2.5. Surface plasmon resonance (SPR) analysis

The interaction between chemical compounds and His-Gα_{i3} or GST-BLT2$_{iL3}$ was analyzed by surface plasmon resonance (SPR) using an SPR imaging instrument (SPRί; K-MAC, Korea). About 1 μM of protein was immobilized on the BK7 sensor chip by incubation at 4 °C for 3 h in PBS buffer. Then, various concentrations of the chemicals in the PBS buffer were applied to the sensor chip with a flow rate of 30 μL per min and then washed with PBS buffer. The resonance unit (RU) was measured during the binding and washing periods, and the binding kinetics were analyzed using SigmaPlot (Systat Software, CA).

2.6. Measurement of cell viability

Cell viability was measured using the 3-(4,5-dimethylthiazol-2-yl)-2,5-diphenyltetrazolium bromide (MTT) assay, which is based on the ability of live cells to convert tetrazolium salt into purple formazan [22]. Briefly, 2×10^4 cells were grown in 96-well plates and incubated for 48 h with purpurin and chloranil at the indicated concentrations. Twenty microlitre of MTT stock solution (5 mg/mL, Sigma–Aldrich) was added to each well and incubated for 4 h at 37 °C in a humidified CO_2 incubator. The supernatant was then removed, and 200 μL of DMSO was added to each well to solubilize the water-insoluble purple formazan crystals. The absorbance at 550 nm was measured using a microplate reader (Molecular Devices, Sunnyvale, CA). All measurements were performed in triplicate.

2.7. SDS-PAGE and immunoblot analysis

Protein samples were heated at 95 °C for 5 min and then analyzed by sodium dodecyl sulfate (SDS) polyacrylamide gel electrophoresis (PAGE) performed on 12% acrylamide gels, followed by transfer to polyvinylidene difluoride (PVDF) membranes using a Hoefer wet transfer unit (for 70 min at 90 V). The membranes were blocked for 1 h with Tris-buffered saline containing 0.05% (v/v) Tween 20 and 5% (w/v) non-fat dry milk, incubated first for 1 h with the primary antibody (1:1000 dilutions for phospho-Akt) in blocking solution, and then for 1 h with horseradish peroxidase (HRP)-conjugated secondary antibody, prior to development using an ECL kit (Amersham Pharmacia, NJ). The hybridized immunoblots were analyzed by autoradiography.

2.8. Chemotaxis assay

Chemotactic motility was assayed using Transwell chambers with 6.5 mm-diameter polycarbonate filters (8 μm pore size, Corning Costar), as previously described [2]. Briefly, the lower surfaces of the filters were coated with 10 μg/mL fibronectin in serum-free RPMI 1640 medium for 1 h at 37 °C. Dry, coated filters containing various amounts of LTB_4 were placed in the lower wells of the Transwell chambers, after which 100 μL of CHO cells stably expressing BLT1 and BLT2 in serum-free RPMI 1640 were loaded into the top wells, yielding a final concentration of 2×10^4 cells/mL. When assessing the effects of inhibitors, cells were pretreated with the respective inhibitor for 30 min before seeding. After incubation at 37 °C in 5% CO_2 for 3 h, the filters were fixed for 3 min with methanol and stained for 10 min with hematoxylin and eosin. Chemotaxis was quantified by counting the cells on the lower side of the filter under an optical microscope (magnification, ×200). Six fields were counted in each assay; each sample was assayed in duplicate; and the assays were repeated twice.

2.9. Rac1 activity assay

Rac1 activation was measured using a GST-PAK-PBD fusion protein that binds GTP-bound, activated Rac1, as previously described [2,23]. Briefly, the fusion was expressed in *E. coli* BL21 cells transformed with the pGEX-4T3 plasmid by IPTG induction and then purified by column chromatography using glutathione-Sepharose-4B. Cells were serum-starved for 24 h and then pretreated with the respective inhibitor for 30 min prior to stimulation with LTB_4 for 5 min. Thereafter, the cell lysates were prepared in lysis buffer (50 mM HEPES, pH 7.4, 10 mM NaF, 75 mM NaCl, 1% Nonidet P-40, 1 mM phenylmethylsulfonyl fluoride, and 1 mM Na_2VO_3) and centrifuged for 30 s at $12000 \times g$, and the supernatant was incubated on ice for 3 min with GST-PAK-PBD fusion protein, which had been freshly coupled to glutathione-agarose beads. Proteins complexed to the beads were recovered by centrifugation, washed three times with lysis buffer, and resuspended in sample buffer. The proteins were separated by 15% SDS-PAGE and transferred to PVDF membranes. The membranes were then probed with anti-Rac1 antibody (1:1000 dilution) and detected using an HRP-conjugated secondary antibody and an ECL detection kit (Amersham Pharmacia).

2.10. Measurement of intracellular H_2O_2

Intracellular H_2O_2 was measured as a function of DCF fluorescence using the procedure described previously [24]. Briefly, 2×10^5 cells were grown in 60 mm dishes and incubated in RPMI 1640 supplemented with 10% FBS for 24 h before measuring ROS. They were then stabilized in serum-free RPMI 1640 without phenol red for at least 2 h before exposure to agonist for the incubated time. To assess the effects of inhibitors, cells were pretreated with the respective inhibitor for 30 min. To measure intracellular H_2O_2, cells were incubated for 40 min in

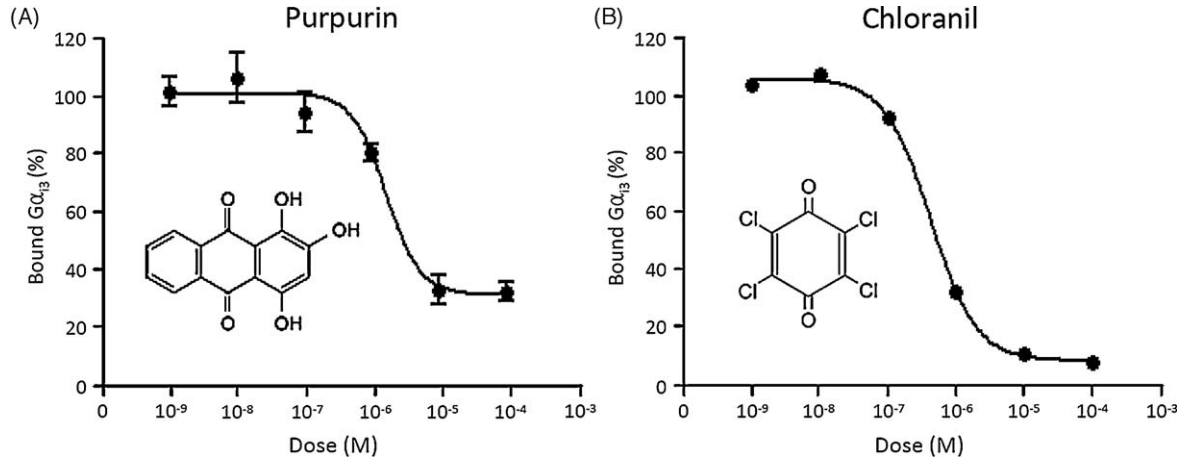

Fig. 2. Inhibitory activity and chemical structure of purpurin and chloranil. FITC-His-$G\alpha_{i3}$ was mixed with various concentrations of purpurin and chloranil. Dose-dependent inhibition curves for these molecules were analyzed by measuring the amount of FITC-His-$G\alpha_{i3}$ specifically bound to the immobilized GST-$BLT2_{iL3}$, and the IC_{50} values were obtained from a nonlinear regression using Prism version 4 (GraphPad software, CA).

the dark at 37 °C in a humidified CO_2 incubator with the H_2O_2-sensitive fluorophore H_2DCFDA (20 μM). H_2DCFDA is hydrolyzed intracellularly to DCF, which is trapped inside the cell. Although H_2DCFDA itself is not fluorescent, it is oxidized in the presence of H_2O_2 to the highly fluorescent DCF. Once loaded with the indicator, the cells were harvested using trypsin-EDTA and resuspended in serum-free RPMI 1640 without phenol red. DCF fluorescence was measured using an FACSCalibur flow cytometer (Becton Dickinson, NJ) with excitation and emission wavelengths of 488 and 530 nm, respectively. Values represent the means ± S.D. of DCF fluorescence from three independent experiments.

2.11. Statistical analysis

All values are expressed as the mean ± standard deviations. Statistical comparison between experimental groups was carried out using Student's *t*-test. Values of $p < 0.01$ were considered statistically significant. Values of $p < 0.01$, $p < 0.001$, and $p < 0.0001$ are designated by *, **, and ***, respectively.

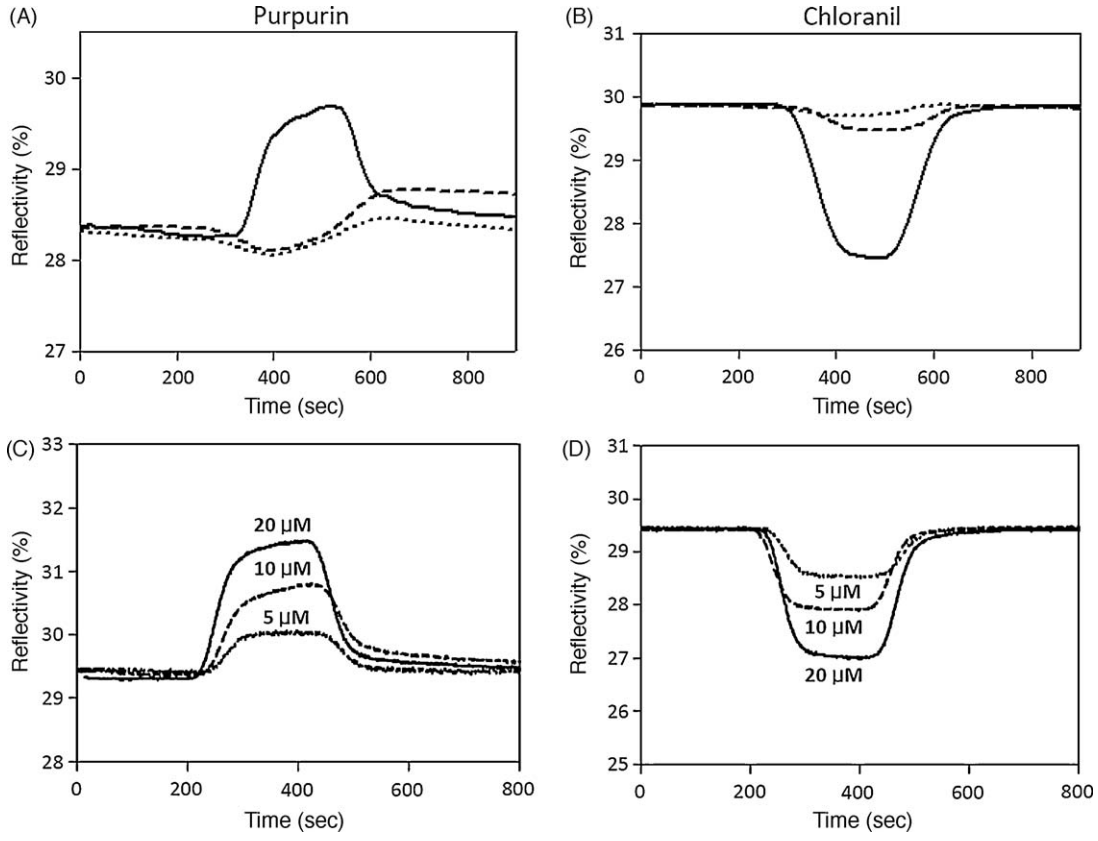

Fig. 3. SPR analysis of purpurin and chloranil binding to $BLT2_{iL3}$ or $G\alpha_{i3}$. The binding sensorgrams of purpurin and chloranil to GST, GST-$BLT2_{iL3}$, or His-$G\alpha_{i3}$, immobilized on the sensor chip, were measured using an SPR imaging instrument. The sensorgrams of purpurin (A) and chloranil (B) binding to GST, GST-$BLT2_{iL3}$, or His-$G\alpha_{i3}$ were obtained at 10 μM concentration and are indicated as dotted, solid, and dashed lines, respectively. The binding kinetics were obtained with 1 μM, 10 μM, and 20 μM purpurin (C) or chloranil (D) and GST-$BLT2_{iL3}$.

3. Results

3.1. Purpurin and chloranil interfere with the interaction of GST-BLT2$_{iL3}$ and His-Gα_{i3}

To screen for compounds that interfere with the interaction of BLT2 and Gα_{i3}, the NINDS chemical library, composed of 1040 FDA-approved drugs and bioactive compounds, was assayed by an *in vitro* system measuring the interaction between the third intracellular loop region of BLT2 (GST-BLT2$_{iL3}$) and Gα_{i3} (FITC-His-Gα_{i3}). From the screening of the library, purpurin and chloranil (Fig. 2) were identified as specific agents that interfered with the interaction of FITC-His-Gα_{i3} with immobilized GST-BLT2$_{iL3}$. The inhibitory activities of these compounds on the interaction between FITC-His-Gα_{i3} and immobilized GST-BLT2$_{iL3}$ were further analyzed at various concentrations. As shown in Fig. 2, both compounds interfere with the interaction between FITC-His-Gα_{i3} and GST-BLT2$_{iL3}$ in the micromolar concentration range. The IC_{50} values of purpurin and chloranil were measured as 1.6 and 0.42 μM, respectively. These results indicated that purpurin and chloranil could specifically interfere with the interaction between BLT2 and Gα_{i3} and might disrupt the signaling pathway of BLT2-dependent cellular responses.

3.2. Purpurin and chloranil bind specifically to BLT2$_{iL3}$ rather than Gα_{i3}

Effective blockade of the interaction between GST-BLT2$_{iL3}$ and His-Gα_{i3} by purpurin and chloranil suggests that these compounds may bind directly to either BLT2$_{iL3}$ or Gα_{i3}. To examine the binding interactions of purpurin and chloranil, the binding kinetics of these chemicals to immobilized GST, GST-BLT2$_{iL3}$, and His-Gα_{i3} were examined via SPR analysis. When purpurin was applied to the GST-BLT2$_{iL3}$, a significant binding sensorgram was observed (Fig. 3A, solid lines), and the binding capacity increased with the concentration of purpurin (Fig. 3C). In contrast, purpurin failed to show any significant binding sensorgram toward the GST control (Fig. 3A, dotted line) or His-Gα_{i3} (Fig. 3A, dashed lines). These results suggest that purpurin binds specifically to the third intracellular loop region of BLT2 rather than Gα_{i3}. In the case of chloranil, the sensorgram was significantly reduced when it was applied to GST-BLT2$_{iL3}$ (Fig. 3B, solid line), and was further reduced as the concentration of chloranil increased (Fig. 3D). This reduced reflectivity is probably due to the mass uptake of chloranil on GST-BLT2$_{iL3}$ [25]. Like purpurin, chloranil failed to show any significant binding to GST or His-Gα_{i3} (Fig. 3B, dotted and dashed lines). These results indicate that chloranil also binds specifically to the third intracellular loop region of BLT2, not to Gα_{i3}. The K_D values of purpurin and chloranil were measured as 3.8 and 1.9 μM, respectively. Together, these results suggest that purpurin and chloranil specifically bind to BLT2$_{iL3}$, thus interfering with BLT2$_{iL3}$ interaction with Gα_{i3} protein.

3.3. Blockade of the BLT2 pathway by purpurin and chloranil inhibits LTB$_4$-induced PI3K/Akt activation

Next, we assessed any effects of purpurin and chloranil on BLT2-signaling in cells. Before the signaling analysis, we examined the cytotoxicity of these compounds in CHO cells using MTT assays. Increasing concentrations (10^{-9}, 10^{-8}, 10^{-7}, 10^{-6}, and 10^{-5} M) of purpurin or chloranil did not affect the viability of CHO cells in 0.5% serum conditions. In addition, the viability of CHO cells treated with two-fold excess doses of the IC_{50} of purpurin and chloranil (3.2 μM and 0.84 μM, respectively) were not affected up to 48 h of treatment (data not shown).

Previously, it was shown that LTB$_4$ treatment transiently induces PI3K/Akt phosphorylation in murine bone marrow-derived mast cells (mBMMCs) and also that LTB$_4$-induced PI3K/Akt phosphorylation is BLT2-dependent in human monocyte-derived DCs [15,26]. We therefore examined whether LTB$_4$-induced Akt activation was inhibited by purpurin and chloranil in CHO-BLT2 stable cells. CHO cells were useful for this study because this cell type does not express any intrinsic receptors for LTB$_4$, as previously revealed by [^{3}H]LTB$_4$ binding assays [1,27]. As shown in Fig. 4, LTB$_4$ elicited significantly enhanced (about 3-fold) Akt phosphorylation in CHO-BLT2 cells, but not in control CHO cells. However, the enhanced Akt phosphorylation in CHO-BLT2 cells was dramatically attenuated by purpurin or chloranil. As positive controls, LY294002 (an inhibitor of PI3K) and PTX (an inhibitor of the Gα_i family) were used, and pretreatment with these inhibitors dramatically reduced the LTB$_4$-induced Akt phosphorylation (Fig. 4). These results suggest that purpurin and chloranil inhibit LTB$_4$-induced PI3K/Akt activation in BLT2-expressing cells.

3.4. Blockade of the BLT2 interaction with Gα_{i3} by purpurin and chloranil inhibits LTB$_4$-induced chemotaxis

It has been reported that PI3K/Akt plays a critical role in various cellular responses, including chemotactic migration in leukocytes [15,28,29]. Similarly, the cellular function of BLT2 is

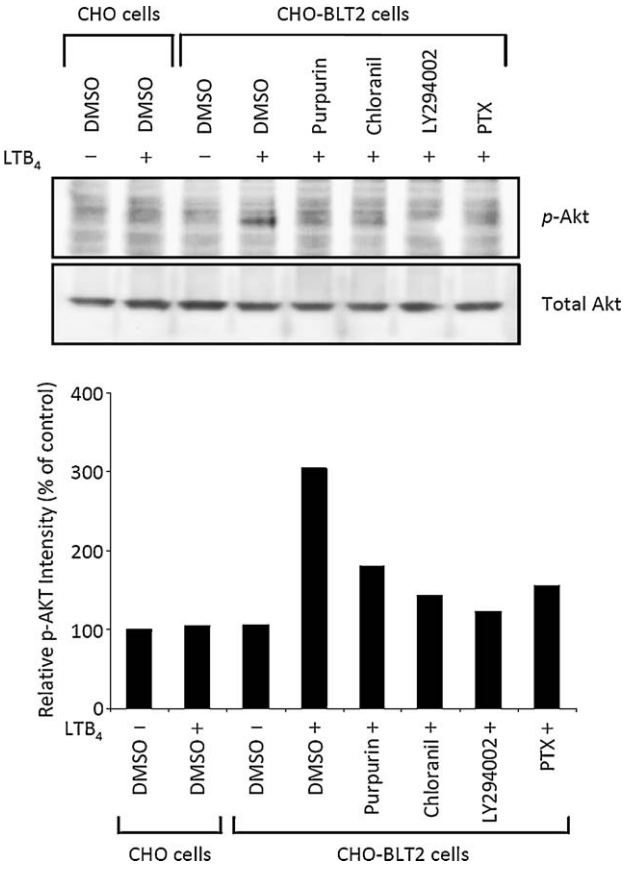

Fig. 4. Effect of purpurin and chloranil on LTB$_4$-induced Akt activation. Serum-starved CHO and CHO-BLT2 stable cells were exposed to LTB$_4$ (300 nM) for 5 min after pretreatment with purpurin (3.2 μM), chloranil (0.84 μM), LY294002 (20 μM), or PTX (100 ng/mL). Each inhibitor was added 30 min prior to the addition of LTB$_4$, with the exception of PTX, which was added 10 h earlier. The cell lysates were analyzed for the level of Akt phosphorylation by SDS-PAGE as described in Section 2. The relative P-Akt intensity was measured and expressed as a percentage of the control.

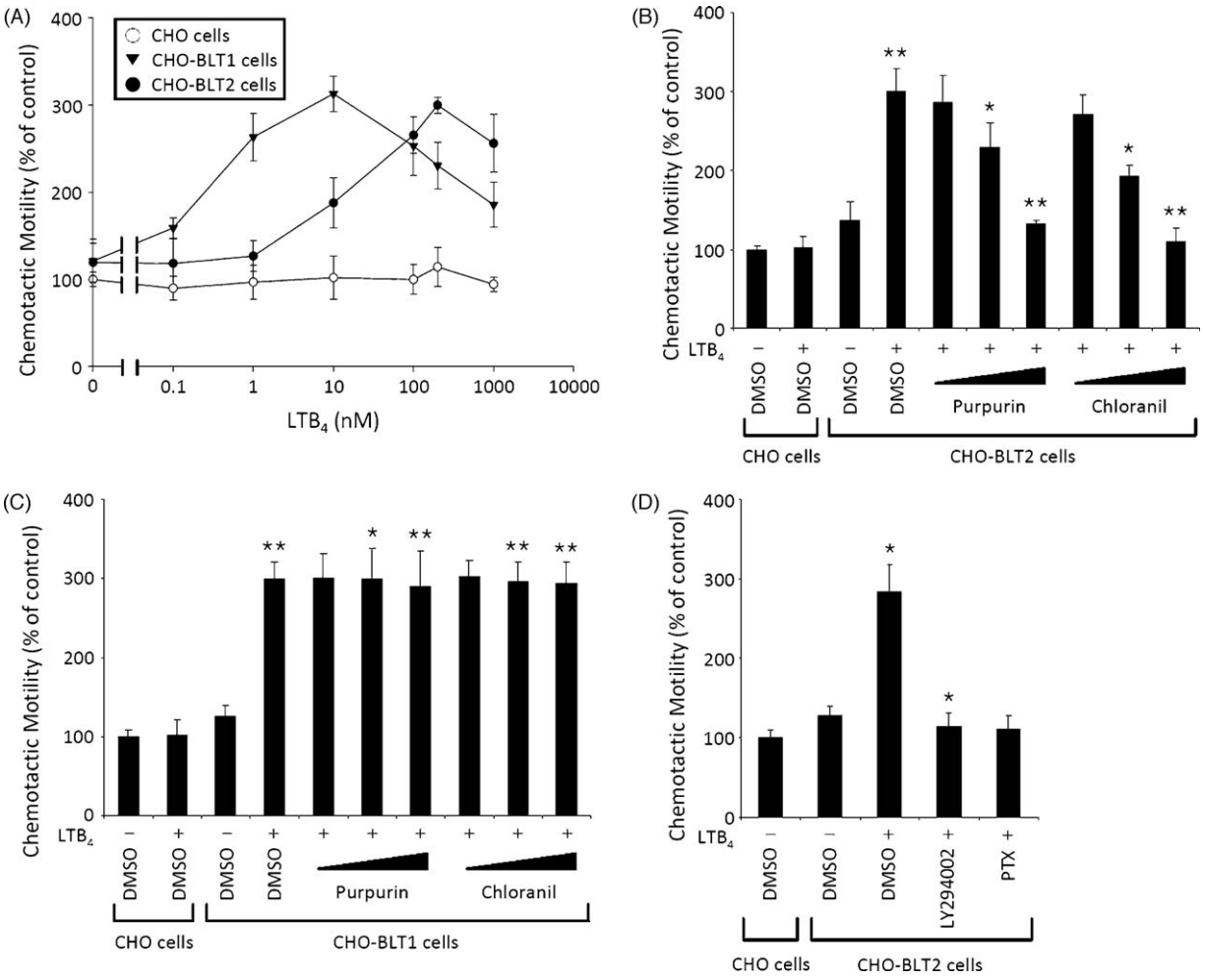

Fig. 5. Inhibitory effects of purpurin and chloranil on LTB_4-induced chemotaxis. (A) Dose dependency of LTB_4-induced chemotactic motility was determined in CHO (○), CHO-BLT1 (▼), and CHO-BLT2 (●) stable cells, as described in Section 2 (B) CHO and CHO-BLT2 cells were preincubated for 30 min with purpurin (0.32, 1.6, and 3.2 μM) or chloranil (0.084, 0.42, and 0.84 μM) prior to exposure to LTB_4 (300 nM). Data are expressed as the mean ± S.D. and are statistically different from the control group at $^{*}p < 0.01$ or $^{**}p < 0.001$. (C) CHO and CHO-BLT1 cells were exposed to LTB_4 (10 nM) for 3 h after pretreatment with purpurin (0.32, 1.6, and 3.2 μM) and chloranil (0.084, 0.42, and 0.84 μM). Each inhibitor was added 30 min prior to the addition of LTB_4. Data are expressed as the mean ± S.D. and are statistically different from the control group at $^{*}p < 0.01$ or $^{**}p < 0.001$. (D) CHO and CHO-BLT2 cells were preincubated with LY294002 (20 μM) for 30 min or with PTX (100 ng/mL) for 10 h prior to exposure to LTB_4 (300 nM) for 3 h. The migrated cell numbers were determined by counting using optical microscopy (A–D). Data are expressed as the mean ± S.D. and are statistically different from the control group at $^{*}p < 0.01$.

known to mediate chemotaxis under the stimulus of LTB_4 [8]. Thus, we next examined whether purpurin and chloranil inhibit LTB_4-induced chemotaxis in CHO-BLT2 cells. As shown in Fig. 5A, chemotactic migration activity was shown with bell-shaped dose response curves to LTB_4 stimuli in both CHO-BLT1 and CHO-BLT2 stable cells, but not in control CHO cells. Furthermore, this chemotactic migration was inhibited by pretreatment with purpurin or chloranil in CHO-BLT2 stable cells in a dose-dependent manner (Fig. 5B). Likewise, the LTB_4-induced chemotaxis was inhibited by LY294002 or PTX treatment in CHO-BLT2 stable cells (Fig. 5D). However, purpurin and chloranil did not show any inhibitory effect on the chemotaxis of CHO-BLT1 cells (Fig. 5C). In fact, the amino acid sequences in the third intracellular loop region of BLT1 and BLT2 are quite different from each other [8], suggesting that the action of these small molecules is quite specific to BLT2. Together, these results indicate that the BLT2-dependent chemotactic migration induced by LTB_4 is inhibited by purpurin and chloranil and that PI3K activity is also required for LTB_4-induced chemotaxis. The inhibitory effect of purpurin and chloranil on LTB_4-induced chemotactic migration was also demonstrated in human umbilical vein endothelial cells (HUVECs), which are primary cells, thus suggesting that the inhibitory effects of purpurin and chloranil on LTB_4-induced chemotaxis are very similar in primary cells (HUVECs) and in the CHO cell line (data not shown).

3.5. Purpurin and chloranil inhibit LTB_4-induced chemotaxis via the Rac1-ROS-linked pathway

Previously, we reported that LTB_4-induced ROS generation is involved in chemotaxis in Rat-2 fibroblast cells [2] and also that ROS generation is through a BLT2-dependent pathway [24]. Furthermore, we and others have reported that Rac1 plays a crucial mediatory role in ROS generation in cells [2,30–32]. We therefore examined the effect of purpurin and chloranil on LTB_4-induced Rac1 activation and ROS generation in CHO-BLT2 cells. To assess whether Rac1 is involved in LTB_4 chemotaxis signaling, we compared the chemotactic effect of LTB_4 in CHO-BLT2 cells and CHO-BLT2-Rac^{N17} cells expressing a dominant negative Rac1 mutant [33]. As shown in Fig. 6A, LTB_4-induced chemotactic migration of CHO-BLT2 stable cells expressing Rac^{N17} was significantly diminished when compared to CHO-BLT2 cells. This result led us to test the extent to which exposure to LTB_4 alters cellular Rac1 activity in CHO-BLT2 cells. Rac1 activity was substantially increased by LTB_4 stimulation in CHO-BLT2 cells

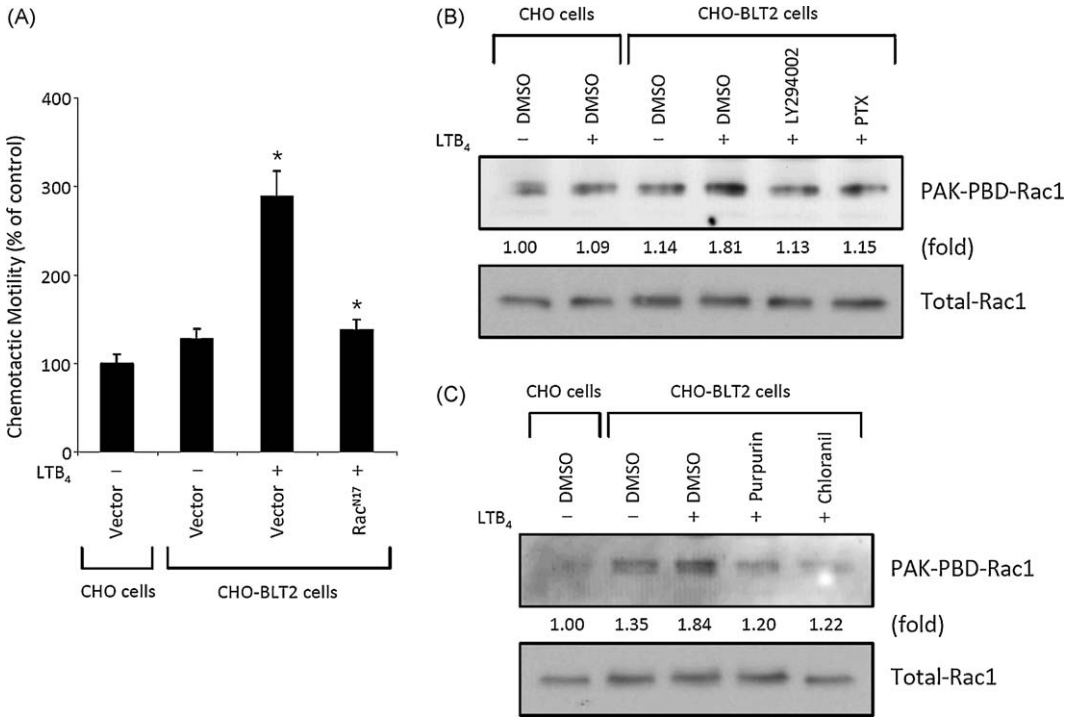

Fig. 6. Purpurin and chloranil inhibit LTB_4-induced Rac1 activation. (A) LTB_4-induced chemotactic motility was analyzed in CHO, CHO-BLT2, and CHO-BLT2-Rac^{N17} stable cells, as described in Section 2. Data are expressed as the mean ± S.D. and are statistically different from the control group at $^*p < 0.01$. (B) CHO and CHO-BLT2 stable cells were serum-starved for 24 h and then preincubated for 30 min with LY294002 (20 μM) or 10 h with PTX (100 ng/mL) prior to exposure to LTB_4 (300 nM) for 5 min. Cell lysates were incubated with GST-PAK-PBD coupled to glutathione-agarose beads. Bound Rac-GTPase was eluted, resolved by 15% SDS-PAGE, and transferred to a PVDF membrane, which was then probed with an anti-Rac1 antibody. (C) CHO and CHO-BLT2 stable cells were serum-starved for 24 h and then preincubated for 30 min with purpurin (3.2 μM) or chloranil (0.84 μM) prior to exposure to LTB_4 (300 nM) for 5 min. LTB_4-induced Rac1 activation was analyzed with these inhibitors as described above. The PAK-PBD-Rac1 intensity was measured and expressed as multiples of the control.

(about 2-fold), but inhibited by LY294002 and PTX (Fig. 6B). As expected, LTB_4-induced Rac1 activation in CHO-BLT2 cells was also inhibited by pretreatment with purpurin or chloranil (Fig. 6C).

Next, we investigated the possible involvement of ROS generation in LTB_4 chemotaxis signaling in CHO-BLT2 cells. As shown in Fig. 7A, LTB_4-induced chemotactic migration was significantly reduced by treatment with NAC, a free radical scavenger, in CHO-BLT2 cells. We next assessed whether LTB_4 treatment induced elevated generation of ROS via the BLT2 pathway. The resultant ROS generation was monitored by DCF fluorescence using a flow cytometer, and the level of ROS generation in CHO-BLT2 cells increased about 2-fold with LTB_4 stimulus (Fig. 7B). This effect was inhibited by pretreatment of CHO-BLT2 stable cells with purpurin or chloranil in a dose-dependent manner (Fig. 7C). Similarly, we observed that LTB_4-induced ROS generation was inhibited by LY294002 or PTX treatment (Fig. 7D), as well as by Rac^{N17} expression in CHO-BLT2 cells (Fig. 7E). Together, these results indicate that purpurin and chloranil inhibit Rac1 activation by LTB_4 signaling and the subsequent ROS generation via the BLT2-dependent pathway. They also suggest that the Rac1-ROS linked cascade plays an important role in the LTB_4-BLT2-evoked chemotactic pathway.

4. Discussion

In the present study, we screened for novel small molecules that could interfere with the interaction between the third intracellular loop region of BLT2 ($BLT2_{iL3}$) and the $G\alpha_{i3}$ protein subunit ($G\alpha_{i3}$), using an HTS assay with a library of 1040 FDA-approved drugs and bioactive compounds, and we identified purpurin and chloranil as specific molecules that blocked the interaction between $BLT2_{iL3}$ and $G\alpha_{i3}$. Further, we demonstrated that these small molecules blocked LTB_4-induced BLT2-dependent chemotaxis. In addition, our findings suggest that purpurin and chloranil could specifically block the activation of LTB_4-BLT2-downstream signaling components (e.g., PI3K/Akt, Rac1, ROS), thus indicating the potential application of these molecules as therapeutic drugs against BLT2-associated inflammatory diseases.

LTB_4 is one of the most potent chemoattractants toward leukocytes such as neutrophils, and it acts via its GPCR receptors, BLT1 and BLT2 [1,8,34]. Although most studies of LTB_4 receptors have been focused on BLT1, it has recently been reported that BLT2 is also involved in many kinds of inflammatory diseases [6,11–13]. In spite of the growing reports on BLT2-associated pathogenesis, however, the detailed cellular mechanism of BLT2 is largely unknown. BLT2 was originally cloned and characterized by Yokomizo et al. [8], who reported at that time that BLT2 was involved in the chemotactic response to LTB_4 [8]. Since then, BLT2-dependent chemotactic responses have been observed in response to a variety of BLT2-specific ligands/agonists (including 12(S)-hydroxyeicosatetraenoic acid [27], Compound A [14], and 12(S)-hydroxyheptadeca-5Z, 8E, 10E-trienoic acid [35]), further suggesting that chemotaxis is an intrinsic activity of BLT2 stimulation. LTB_4-induced chemotaxis was shown to be completely inhibited by pretreatment with PTX, suggesting that BLT2-mediated chemotaxis is associated with a $G\alpha_i$ family member [8]. In accordance with this idea, we previously reported that the third intracellular loop region of BLT2 interacts with $G\alpha_{i3}$ [16]. Therefore, the binding of $BLT2_{iL3}$ and $G\alpha_{i3}$ may play a role in the LTB_4-induced intracellular signaling pathway leading to chemotaxis. Like LTB_4, many chemoattractants are known to interact with G-protein coupled chemoattractant receptors to elicit a number of biological functions, including chemotaxis, trafficking, and homing of leukocytes [21,36,37].

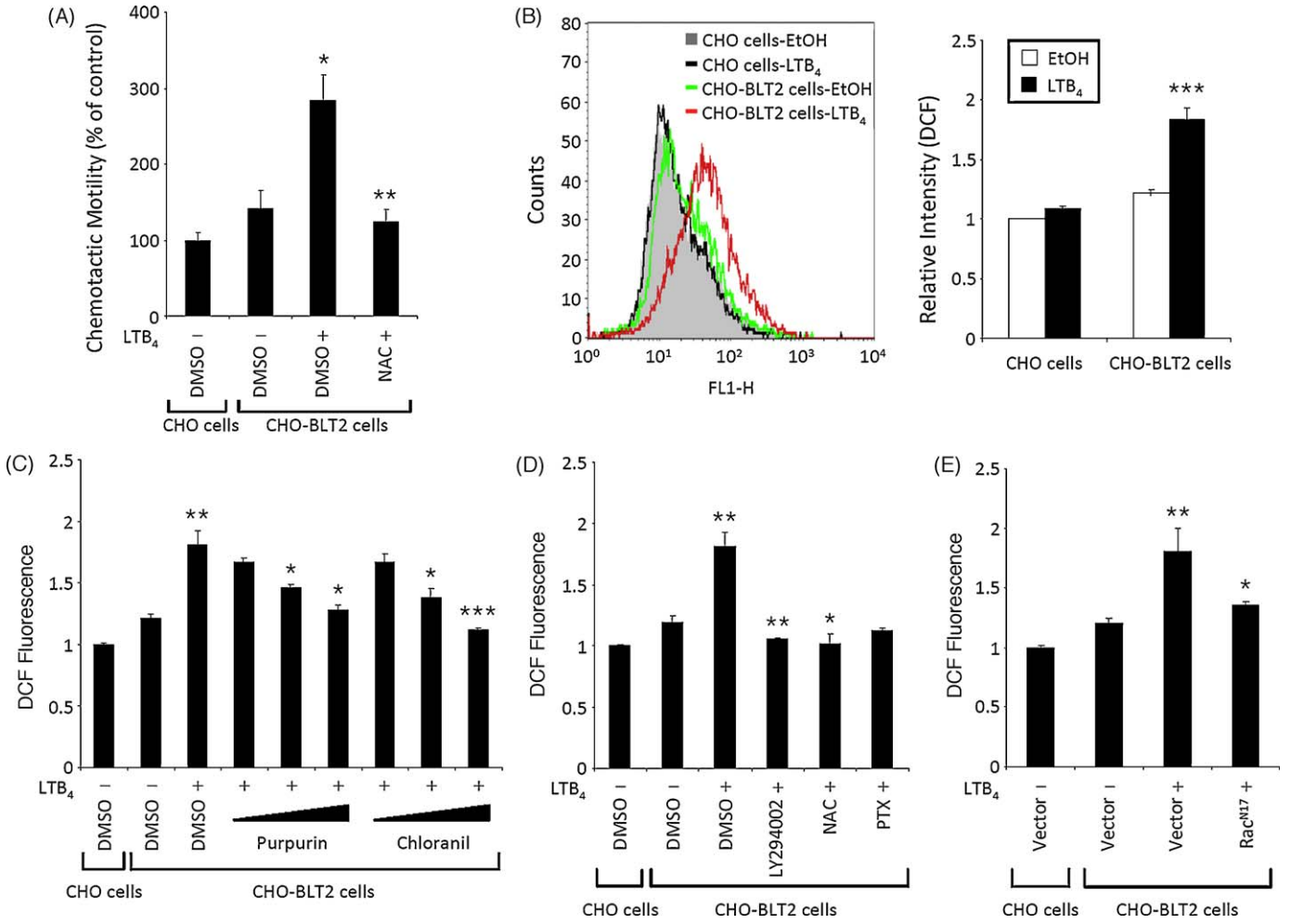

Fig. 7. Purpurin and chloranil inhibit LTB_4-induced ROS generation. (A) LTB_4-induced chemotactic motility was analyzed after pretreatment with NAC (2 mM) for 30 min in CHO and CHO-BLT2 stable cells, as described in Section 2. Data are expressed as the mean ± S.D. and are statistically different from the control group at $^{*}p < 0.01$ or $^{**}p < 0.001$. (B) CHO and CHO-BLT2 stable cells were stabilized in serum-free RPMI 1640 without phenol red for at least 2 h prior to exposure to LTB_4 (300 nM), after which DCF fluorescence was monitored with a flow cytometer. Data are expressed as the mean ± S.D. and are statistically different from the control group at $^{***}p < 0.0001$. (C and D) Serum-starved CHO and CHO-BLT2 stable cells were exposed to LTB_4 (300 nM) after pretreatment with purpurin (0.32, 1.6, and 3.2 μM), chloranil (0.084, 0.42, and 0.84 μM), LY294002 (20 μM), NAC (2 mM), or PTX (100 ng/mL). Inhibitors were added 30 min (or 10 h in case of PTX) prior to the addition of LTB_4. Data are expressed as the mean ± S.D. and are statistically different from the control group at $^{*}p < 0.01$, $^{**}p < 0.001$, or $^{***}p < 0.0001$. (E) Serum-starved CHO, CHO-BLT2, and CHO-BLT2-Rac^{N17} cells were exposed to LTB_4 (300 nM). Data are expressed as the mean ± S.D. and are statistically different from the control group at $^{*}p < 0.01$ or $^{**}p < 0.001$. DCF fluorescence levels, reflecting the relative levels of ROS (arbitrary units), were quantified as described in Section 2 (B–E).

Chemotaxis is involved in diverse pathological inflammatory conditions [38] and is a complex and orchestrated cellular phenomenon that is mediated by specific intracellular signaling pathways [38]. In particular, Akt was shown to be involved in chemotaxis in response to a variety of chemoattractants [21,38]. This kinase plays a critical role in chemotaxis evoked through the activation of GPCRs that are coupled to $G\alpha_i$s of the heterotrimeric G-protein family. Further, the Gβγ subunits released from $G\alpha_i$ heterotrimers upon chemotactic receptor activation are suggested to initiate signaling events leading to chemotaxis by activating PI3K-γ and subsequently Akt [39,40]. More recently, Ayoub et al. showed that blockade of the Gα subunit inhibits heterotrimeric G-protein-mediated chemotactic signaling, thus preventing the downstream signaling cascade [41]. Together, it is likely that chemotactic GPCR receptors depend on activation of PI3K and Akt to initiate the chemotactic signaling cascade. Consistent with this idea, we also found that Akt is involved in the LTB_4-induced chemotactic signaling pathway in CHO-BLT2 cells (Fig. 4). In addition, we identified Rac1 and ROS as further downstream components in the LTB_4-induced pathway to chemotaxis in CHO-BLT2 cells, which is consistent with our previous report suggesting that an 'Rac1-ROS' cascade is essential for the LTB_4-induced chemotaxis in Rat-2 fibroblasts [2]. On the basis of these results, we propose the model summarized in Fig. 8. In this model, we propose that purpurin and chloranil interfere with the BLT2-$G\alpha_{i3}$ interaction which is critical for the stimulation of the LTB_4-induced BLT2-chemotactic downstream (PI3K/Akt, Rac1, and ROS) pathway (Fig. 8).

The NINDS library was screened in the present study in order to identify potential molecules that could interfere with the interaction between $BLT2_{iL3}$ and $G\alpha_{i3}$. Screening of FDA-approved compound collections has many advantages over that of conventional small molecule chemical libraries. For example, the conventional approach (e.g., from preclinical validation to FDA approval) for developing a new drug takes a long time and is expensive; FDA approval of a new drug takes an average of 12 years, and the odds of a new drug becoming approved are approximately one in 5000. In contrast, the FDA-approved compounds used in the present study have proven clinical drug properties, including data on solubility, cell permeability, and toxicity, making it possible to bypass some drug development steps and move directly to identifying "ideal" candidate

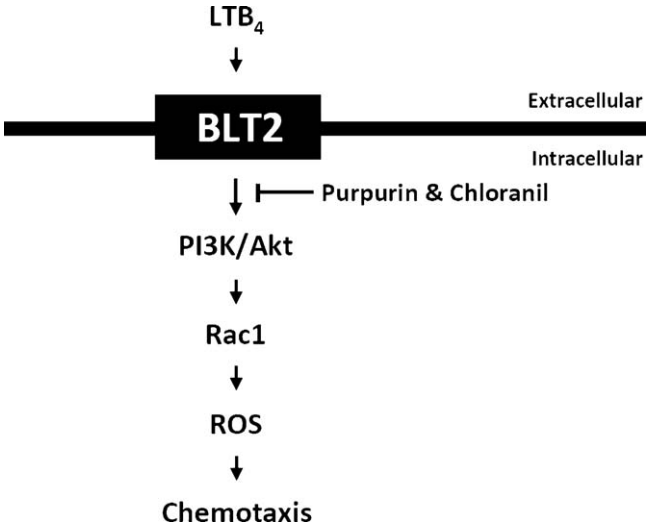

Fig. 8. Schematic model for the role of purpurin and chloranil as BLT2 inhibitors. LTB_4 binding to BLT2 results in the activation of the $G\alpha_i$-dependent pathway, which subsequently stimulates PI3K/Akt phosphorylation. Activation of PI3K/Akt leads to Rac1 activation and subsequent ROS generation, leading to chemotactic motility. Purpurin and chloranil, which bind to the third intracellular loop region of BLT2, interfere with the BLT2-$G\alpha_{i3}$ interaction, thus suppressing LTB_4-induced chemotactic motility.

therapeutic agents as already defined [20]. The application of the NINDS library to GPCRs-based drug discovery is especially advantageous, and, to our knowledge, the present study is the first report to target the NINDS library to GPCRs. By employing a similar screening scheme to target the GPCR-G-protein interaction, as described in the present study, it is expected that various valuable novel pharmacological drug candidates will be identified. In fact, it is well known that GPCRs are the single largest drug target, representing 25–50% of marketed clinical drugs prescribed today in the United States [42].

In the present study, we identified purpurin and chloranil as potential BLT2-blocking pharmacological candidates via a NINDS library screen. Purpurin is a naturally occurring yellow-colored anthraquinone pigment isolated from a species of madder root (*Rubia tinctorum*). Although it has been reported that purpurin shows anti-cancer activity [43–45] and it acted against human cytochrome P450 and NADPH-cytochrome P450 reductase [46], the exact mechanism of action by which purpurin demonstrates these activities remains unknown, especially regarding its action through GPCRs. Similarly, although chloranil has traditionally been used as a fungicide or oxidizing agent in organic synthesis, and has also been shown to be effective in psoriasis treatment [47], the exact mechanism of its action remains unknown. From the present results, we suspect that the working mechanisms by which purpurin and chloranil demonstrate their effective therapeutic healing activities are likely to be mediated through GPCRs, especially BLT2, and future studies will be necessary to investigate the potential signaling association between these compounds and BLT2 in each effective therapeutic action mechanism. In addition, future studies aimed at investigating the efficacy of these small compounds toward BLT2-associated inflammatory diseases such as asthma are necessary.

In summary, we screened a library composed of FDA-approved drugs and bioactive compounds for potential BLT2 blockers and identified two small molecules, purpurin and chloranil, that interfere with the interaction between the third intracellular loop region of BLT2 ($BLT2_{iL3}$) and the Gα subunit of type i3 ($G\alpha_{i3}$). Furthermore, our findings indicate that these molecules inhibited BLT2-downstream components (e.g., PI3K/Akt, Rac1, and ROS), thus blocking LTB_4-BLT2-evoked chemotaxis. We propose that purpurin and chloranil may be regarded as BLT2-blocking pharmacological molecules available as therapeutic agents against BLT2-associated inflammatory human diseases.

Acknowledgments

This work was supported by the Diseases Network Research Program (M10751050004-08N5105-00410) (to J-H.K), the 21C Frontier Research Program (FPR05B2040) (to Y-G.Y) from the Ministry of Education, Science & Technology, South Korea, and the Korea Research Foundation Grant funded by the Korean Government (MOEHRD, Basic Research Promotion Fund) (KRF-2008-3130C00603) (to J-H.K). We thank to Dr. Takao Shimizu (University of Tokyo, Tokyo, Japan) and Dr. Takehiko Yokomizo (University of Kyushu, Fukuoka, Japan) for the BLT1 expression plasmids, and Dr. Young-Chul Choi (Kyung Hee University, Korea) for the BAC library.

References

[1] Yokomizo T, Izumi T, Chang K, Takuwa Y, Shimizu T. A G-protein coupled receptor for leukotriene B4 that mediates chemotaxis. Nature 1997;387:620–4.
[2] Woo CH, You HJ, Cho SH, Eom YW, Chun JS, Yoo YJ, et al. Leukotriene B(4) stimulates Rac-ERK cascade to generate reactive oxygen species that mediates chemotaxis. J Biol Chem 2002;277:8572–8.
[3] Chen XS, Sheller JR, Johnson EN, Funk CD. Role of leukotrienes revealed by targeted disruption of the 5-lipoxygenase gene. Nature 1994;372:179–82.
[4] Turner CR, Breslow R, Conklyn MJ, Andresen CJ, Patterson DK, Lopez-Anaya A, et al. In vitro and in vivo effects of leukotriene B4 antagonism in a primate model of asthma. J Clin Invest 1996;97:381–7.
[5] Griffiths RJ, Pettipher ER, Koch K, Farrell CA, Breslow R, Conklyn MJ, et al. Leukotriene B4 plays a critical role in the progression of collagen-induced arthritis. Proc Natl Acad Sci USA 1995;92:517–21.
[6] Sanchez-Galan E, Gomez-Hernandez A, Vidal C, Martin-Ventura JL, Blanco-Colio LM, Munoz-Garcia B, et al. Leukotriene B4 enhances the activity of nuclear factor-kappaB pathway through BLT1 and BLT2 receptors in atherosclerosis. Cardiovasc Res 2009;81:216–25.
[7] Sharon P, Stenson WF. Enhanced synthesis of leukotriene B4 by colonic mucosa in inflammatory bowel disease. Gastroenterology 1984;86:453–60.
[8] Yokomizo T, Kato K, Terawaki K, Izumi T, Shimizu T. A second leukotriene B(4) receptor, BLT2. A new therapeutic target in inflammation and immunological disorders. J Exp Med 2000;192:421–32.
[9] Kim ND, Chou RC, Seung E, Tager AM, Luster AD. A unique requirement for the leukotriene B4 receptor BLT1 for neutrophil recruitment in inflammatory arthritis. J Exp Med 2006;203:829–35.
[10] Kamohara M, Takasaki J, Matsumoto M, Saito T, Ohishi T, Ishii H, et al. Molecular cloning and characterization of another leukotriene B4 receptor. J Biol Chem 2000;275:27000–4.
[11] Cho KJ, Seo JM, Shin Y, Yoo MH, Park CS, Lee SH, et al. Blockade of airway inflammation and hyperresponsiveness by inhibition of BLT2, a low-affinity leukotriene B4 receptor. Am J Respir Cell Mol Biol 2009.
[12] Hennig R, Osman T, Esposito I, Giese N, Rao SM, Ding XZ, et al. BLT2 is expressed in PanINs, IPMNs, pancreatic cancer and stimulates tumour cell proliferation. Br J Cancer 2008;99:1064–73.
[13] Kim GY, Lee JW, Cho SH, Seo JM, Kim JH. Role of the low-affinity leukotriene B4 receptor BLT2 in VEGF-induced angiogenesis. Arterioscler Thromb Vasc Biol 2009;29:915–20.
[14] Iizuka Y, Yokomizo T, Terawaki K, Komine M, Tamaki K, Shimizu T. Characterization of a mouse second leukotriene B4 receptor, mBLT2: BLT2-dependent ERK activation and cell migration of primary mouse keratinocytes. J Biol Chem 2005;280:24816–23.
[15] Shin EH, Lee HY, Bae YS. Leukotriene B4 stimulates human monocyte-derived dendritic cell chemotaxis. Biochem Biophys Res Commun 2006;348:606–11.
[16] Vukoti KM, Lee WK, Kim HJ, Kim IY, Yang EG, Lee C, et al. Molecular dissection of the interaction between hBLT2 and the G-protein alpha subunits. Bull Korean Chem Soc 2007;28:1005–9.
[17] Desai UA, Pallos J, Ma AA, Stockwell BR, Thompson LM, Marsh JL, et al. Biologically active molecules that reduce polyglutamine aggregation and toxicity. Hum Mol Genet 2006;15:2114–24.
[18] Rothstein JD, Patel S, Regan MR, Haenggeli C, Huang YH, Bergles DE, et al. Beta-lactam antibiotics offer neuroprotection by increasing glutamate transporter expression. Nature 2005;433:73–7.
[19] Chevillet JR, Park GJ, Bedalov A, Simon JA, Vasioukhin VI. Identification and characterization of small-molecule inhibitors of hepsin. Mol Cancer Ther 2008;7:3343–51.
[20] Ou HC, Cunningham LL, Francis SP, Brandon CS, Simon JA, Raible DW, et al. Identification of FDA-approved drugs and bioactives that protect hair cells in the Zebrafish (*Danio rerio*) lateral line and mouse (*Mus musculus*) utricle. J Assoc Res Otolaryngol 2009.

[21] Haribabu B, Zhelev DV, Pridgen BC, Richardson RM, Ali H, Snyderman R. Chemoattractant receptors activate distinct pathways for chemotaxis and secretion. Role of G-protein usage. J Biol Chem 1999;274:37087–92.
[22] Kim JE, Kwon JY, Lee DE, Kang NJ, Heo YS, Lee KW, et al. MKK4 is a novel target for the inhibition of tumor necrosis factor-alpha-induced vascular endothelial growth factor expression by myricetin. Biochem Pharmacol 2009;77:412–21.
[23] Akasaki T, Koga H, Sumimoto H. Phosphoinositide-3 kinase-dependent and -independent activation of the small GTPase Rac2 in human neutrophils. J Biol Chem 1999;274:18055–9.
[24] Choi JA, Kim EY, Song H, Kim C, Kim JH. Reactive oxygen species are generated through a BLT2-linked cascade in Ras-transformed cells. Free Radical Biol Med 2008;44:624–34.
[25] Hook F, Kasemo B, Nylander T, Fant C, Sott K, Elwing H. Variations in coupled water, viscoelastic properties, and film thickness of a Mefp-1 protein film during adsorption and cross-linking: a quartz crystal microbalance with dissipation monitoring, ellipsometry, and surface plasmon resonance study. Anal Chem 2001;73:5796–804.
[26] Lundeen KA, Sun B, Karlsson L, Fourie AM. Leukotriene B4 receptors BLT1 and BLT2: expression and function in human and murine mast cells. J Immunol 2006;177:3439–47.
[27] Yokomizo T, Kato K, Hagiya H, Izumi T, Shimizu T. Hydroxyeicosanoids bind to and activate the low-affinity leukotriene B4 receptor, BLT2. J Biol Chem 2001;276:12454–9.
[28] Puri KD, Doggett TA, Huang CY, Douangpanya J, Hayflick JS, Turner M, et al. The role of endothelial PI3Kgamma activity in neutrophil trafficking. Blood 2005;106:150–7.
[29] Hannigan M, Zhan L, Li Z, Ai Y, Wu D, Huang CK. Neutrophils lacking phosphoinositide-3 kinase gamma show loss of directionality during *N*-formyl-Met-Leu-Phe-induced chemotaxis. Proc Natl Acad Sci USA 2002;99:3603–8.
[30] Woo CH, Eom YW, Yoo MH, You HJ, Han HJ, Song WK, et al. Tumor necrosis factor-alpha generates reactive oxygen species via a cytosolic phospholipase A2-linked cascade. J Biol Chem 2000;275:32357–62.
[31] Sundaresan M, Yu ZX, Ferrans VJ, Sulciner DJ, Gutkind JS, Irani K, et al. Regulation of reactive oxygen species generation in fibroblasts by Rac1. Biochem J 1996;318(Pt 2):379–82.
[32] Woo CH, Lee ZW, Kim BC, Ha KS, Kim JH. Involvement of cytosolic phospholipase A2, and the subsequent release of arachidonic acid, in signaling by Rac for the generation of intracellular reactive oxygen species in rat-2 fibroblasts. Biochem J 2000;348(Pt 3):525–30.
[33] Kim BC, Yi JY, Yi SJ, Shin IC, Ha KS, Jhun BH, et al. Rac-GTPase activity is essential for EGF-induced mitogenesis. Mol Cells 1998;8:90–5.
[34] Kim C, Kim JY, Kim JH. Cytosolic phospholipase A(2), lipoxygenase metabolites, and reactive oxygen species. BMB Rep 2008;41:555–9.
[35] Okuno T, Iizuka Y, Okazaki H, Yokomizo T, Taguchi R, Shimizu T. 12(S)-Hydroxyheptadeca-5Z, 8E, 10E-trienoic acid is a natural ligand for leukotriene B4 receptor 2. J Exp Med 2008;205:759–66.
[36] Baggiolini M. Chemokines and leukocyte traffic. Nature 1998;392:565–8.
[37] Gerard C, Gerard NP. The pro-inflammatory seven-transmembrane segment receptors of the leukocyte. Curr Opin Immunol 1994;6:140–5.
[38] Lee MJ, Thangada S, Paik JH, Sapkota GP, Ancellin N, Chae SS, et al. Akt-mediated phosphorylation of the G-protein coupled receptor EDG-1 is required for endothelial cell chemotaxis. Mol Cell 2001;8:693–704.
[39] Neptune ER, Bourne HR. Receptors induce chemotaxis by releasing the beta-gamma subunit of Gi, not by activating Gq or Gs. Proc Natl Acad Sci USA 1997;94:14489–94.
[40] Stephens L, Smrcka A, Cooke FT, Jackson TR, Sternweis PC, Hawkins PT. A novel phosphoinositide-3 kinase activity in myeloid-derived cells is activated by G-protein beta gamma subunits. Cell 1994;77:83–93.
[41] Ayoub MA, Damian M, Gespach C, Ferrandis E, Lavergne O, De Wever O, et al. Inhibition of heterotrimeric G-protein signaling by a small molecule acting on Galpha subunit. J Biol Chem 2009.
[42] Overington JP, Al-Lazikani B, Hopkins AL. How many drug targets are there? Nat Rev Drug Discov 2006;5:993–6.
[43] Morgan AR, Garbo GM, Kreimer-Birnbaum M, Keck RW, Chaudhuri K, Selman SH. Morphological study of the combined effect of purpurin derivatives and light on transplantable rat bladder tumors. Cancer Res 1987;47:496–8.
[44] Mori H, Ohnishi M, Kawamori T, Sugie S, Tanaka T, Ino N, et al. Toxicity and tumorigenicity of purpurin, a natural hydroxanthraquinone in rats: induction of bladder neoplasms. Cancer Lett 1996;102:193–8.
[45] Di Stefano A, Ettorre A, Sbrana S, Giovani C, Neri P. Purpurin-18 in combination with light leads to apoptosis or necrosis in HL60 leukemia cells. Photochem Photobiol 2001;73:290–6.
[46] Takahashi E, Fujita K, Kamataki T, Arimoto-Kobayashi S, Okamoto K, Negishi T. Inhibition of human cytochrome P450 1B1, 1A1 and 1A2 by antigenotoxic compounds, purpurin and alizarin. Mutat Res 2002;508:147–56.
[47] Teichmann WO, Horvath PN. Chloranil in the treatment of psoriasis; a substitute for chrysarobin. South Med J 1957;50:1521–3.